Composition and diversity of mucosa-associated microbiota along the entire length of the pig gastrointestinal tract; dietary influences.

Jennifer Kelly,[1] Kristian Daly,[1] Andrew W. Moran,[1] Sheila Ryan,[1] David Bravo,[2] Soraya P. Shirazi-Beechey[1]

[1]Department of Functional and Comparative Genomics, Institute of Integrative Biology, University of Liverpool, Liverpool L69 7ZB, UK, [2]Pancosma SA, Voie-des-Traz 6, Le Grand-Sacconex, Geneva, Switzerland, CH 1218

Corresponding Author: Soraya P Shirazi-Beechey, Department of Functional and Comparative Genomics, Institute of Integrative Biology, University of Liverpool, Liverpool L69 7ZB, UK; spsb@liverpool.ac.uk; +44(0)151 794 4255

Running Title: Swine mucosa-associated gut microbiota

This article has been accepted for publication and undergone full peer review but has not been through the copyediting, typesetting, pagination and proofreading process which may lead to differences between this version and the Version of Record. Please cite this article as an 'Accepted Article', doi: 10.1111/1462-2920.13619

Originality-Significance Statement

This paper shows that diet modulates mucosa-associated microbiota along the entire length of the intestinal tract. This opens up the possibility of using dietary strategies to modify mucosa-associated microbiota preventing bacterial-associated gut disorders.

This article has been accepted for publication and undergone full peer review but has not been through the copyediting, typesetting, pagination and proofreading process which may lead to differences between this version and the Version of Record. Please cite this article as an 'Accepted Article', doi: 10.1111/1462-2920.13619

Summary

Mucosa-associated microbial populations of the gastrointestinal tract are in intimate contact with the outer mucus layer. This proximity offers these populations a higher potential, than lumenal microbiota, in exerting effects on the host. Functional characteristics of the microbiota and influences of host- physiology shape the composition and activity of the mucosa-associated bacterial community. We have shown previously that inclusion of an artificial sweetener, SUCRAM, included in the diet of weaning piglets modulates the composition of lumenal-residing gut microbiota and reduces weaning-related gastrointestinal disorders. In this study, using Illumina sequencing we characterised the mucosa-associated microbiota along the length of the intestine of piglets, and determined the effect of SUCRAM supplementation on mucosa-associated populations. There were clear distinctions in the composition of mucosa-associated microbiota, between small and large intestine, concordant with differences in regional oxygen distribution and nutrient provision by the host. There were significant differences in the composition of mucosa-associated compared to lumenal microbiota in pig caecum. Dietary supplementation with SUCRAM affected mucosa-associated bacterial community structure along the length of the intestinal tract. Most notably, there was a substantial reduction in predominant *Campylobacter* populations proposing that SUCRAM supplementation of swine diet has potential for reducing meat contamination and promoting food safety.

This article has been accepted for publication and undergone full peer review but has not been through the copyediting, typesetting, pagination and proofreading process which may lead to differences between this version and the Version of Record. Please cite this article as an 'Accepted Article', doi: 10.1111/1462-2920.13619

Introduction

The microbiota of the gastrointestinal tract has profound influence on host nutrition, immune stimulation, and protection against pathogens. Perturbations in the stability of gut microbial population disposes the host to enteric disorders, pathogenic invasion and disease (Macfarlane *et al*., 2009; Sartor and Mazmanian, 2012). Understanding gut microbial community structure and population dynamics in symbiosis and dysbiosis is fundamental in developing strategies to ameliorate enteric disorders and promoting the establishment of a more beneficial gut-microbiota ecosystem.

Recent developments in molecular biological techniques, such as next-generation sequencing, have transformed the way in which microbial ecosystems can be studied, providing highly detailed information on diverse bacterial populations in different environments. Using these approaches extensive studies have been carried out to characterise gut microbiota, mainly employing faecal samples. Relatively little work has been done on the microbiota present in more proximal regions of the gut or those living within the outer mucosal layer, which may be dissimilar to the faecal microbiota. Moreover, whilst effects of diet/dietary supplements on gut microbiota have become evident, investigations into dietary influence on mucosa-associated microbiota are few (Zoetendal *et al*., 2002; Bik *et al*., 2006; Ahmed *et al*., 2007; Mann *et al*., 2014; Daly *et al*., 2016).

Environmental conditions throughout the mammalian gastrointestinal tract vary longitudinally (proximal to distal) and radially (mucosa to lumen), creating a range of divergent microenvironments, each supporting distinct microbial populations (Stearns *et al*., 2011; Zhao *et al*., 2015). The small intestine is characterised by increased oxygen levels (He *et al*., 1999), antimicrobials (Bevins and Salzman, 2011) and a faster transit time (Schwarz *et al*., 2002) in comparison to the large intestine. In the small intestine, there is also an abundance of simple carbohydrates for which the bacteria and host are in direct competition (Zoetendal *et al*., 2012). Substrate availability in the colon comprises

This article has been accepted for publication and undergone full peer review but has not been through the copyediting, typesetting, pagination and proofreading process which may lead to differences between this version and the Version of Record. Please cite this article as an 'Accepted Article', doi: 10.1111/1462-2920.13619

mainly of complex carbohydrates, such as non-starch polysaccharides, that resist digestion in the small intestine.

Furthermore, the ecosystem within the outer mucosal layer is distinct from that in the lumen. A steep declining oxygen gradient exists from the mucosal tissue into the lumen, creating a microenvironment within the mucosa which is often enriched with oxygen-tolerant populations (Albenberg *et al*., 2014). The abundance of mucin glycoproteins (McGuckin *et al*., 2011) and the close proximity to host tissue also provides mucosa-associated bacteria with additional nutrient sources. This close interaction between host and bacteria also offers the mucosal microbial community with a higher potential to exert effects on the host than lumenal populations. It has been suggested that this community provides a line of defence against pathogens, modulates the immune system and contributes to gut-brain communication (Leser and Molbak, 2009; Macfarlane *et al*., 2011).

In this study we have characterised the profile of the mucosa- associated microbiota along the length of the intestine in early weaned piglets and have assessed similarities/differences between mucosal and lumenal populations. Commercially, piglets are weaned as early as 28 days to increase pig production. However, an immature intestinal immune system disposes them to enteric disorders and increased mortality (Konstantinov *et al*., 2006; Lallès *et al*., 2007). Supplementation of the piglets diet with the artificial sweetener, SUCRAM [consisting of neohesperidin dihydrochalcone (NHDC) and saccharin], increases the population abundance of beneficial *Lactobacillus* species in the lumenal contents (Daly *et al*., 2015) reducing the prevalence of enteric disease (Sterk *et al*., 2008). Here, we have determined the effect of SUCRAM on the mucosa-associated gut microbiota of piglets weaned to a diet supplemented with this artificial sweetener.

We show that mucosa-associated microbiota along the longitudinal axis of the small and large intestine is dominated by Bacteroidetes, Firmicutes and Proteobacteria. Duodenal- and jejunal-

associated microbial communities were almost exclusively prevailed by Proteobacteria, principally by OTUs relating to *Campylobacter coli* and *Helicobacter rappini*. In contrast, Bacteroidetes and Firmicutes, present at relatively low levels in the duodenum and jejunum, steadily increased in abundance along the length of the intestine, becoming dominant phyla within the proximal colon. Moreover, we demonstrate population differences between mucosa-associated and lumenal communities and report on the effects of dietary supplementation with SUCRAM, particularly on predominant populations of *Campylobacter coli*. The latter finding proposes the potential of using dietary strategies to modify mucosa-attached microbiota with attendant promise to prevent bacterial associated gut disorders.

This article has been accepted for publication and undergone full peer review but has not been through the copyediting, typesetting, pagination and proofreading process which may lead to differences between this version and the Version of Record. Please cite this article as an 'Accepted Article', doi: 10.1111/1462-2920.13619

Results

Characterization of pig intestinal mucosa-associated microbiota

To investigate the community structure and diversity of pig intestinal mucosa-associated microbiota, DNA was extracted from mucosal scrapings taken from duodenum, jejunum, ileum, caecum, proximal colon and distal colon of 28-day old piglets weaned to a defined basal diet (BD) and maintained on this diet for a period of two weeks (see Materials and methods for animals and Daly *et al*., 2015 for dietary composition).

Illumina MiSeq sequencing of 16S rRNA gene amplicons, encompassing the hypervariable V4 region, was employed to describe the composition and diversity of the mucosa-associated microbial community (Illumina sequencing data has been deposited in the European Nucleotide Archive (ENA) under project accession number PRJEB14756). The average number of assembled sequence reads per sample was over 400,000, with a mean read length of 250 bp. Rarefaction analysis revealed plateauing curves for all samples, indicating that the majority of microbial diversity within the pig gastrointestinal mucosa had been sufficiently captured. Using a dissimilarity threshold of 3% sequence divergence to classify operational taxonomic units (OTUs) and a relative abundance threshold of 0.01%, we were able to identify 383 distinct OTUs residing within the intestinal mucosa of these pigs.

Phylum-level analysis of the pig mucosa-associated microbiota revealed that all regions of the intestinal tract were dominated by three major bacterial phyla, Bacteroidetes, Firmicutes and Proteobacteria (Fig. 1A). Although ubiquitously dominant within the intestinal tract, each of the three phyla exhibited distinct profiles along the length of the intestine (Fig. 1B). Duodenal and jejunal-mucosa-associated microbial communities were almost exclusively dominated by Proteobacteria (mean abundance 81% and 80% respectively). In the ileum and the large intestine however, the levels of Proteobacteria reduced dramatically, albeit still comprising major populations, reaching their lowest levels in the proximal colon (mean 27% of total) (Fig. 1B). Bacteroidetes and

Firmicutes displayed an opposite profile to Proteobacteria, being present at relatively low levels in the duodenum (mean 5% and 13% respectively), then steadily increasing longitudinally throughout each gut section of the small and large intestine to become the dominant phyla within the proximal colon (35% and 36% on average respectively) (Fig. 1B). Notably, all three phyla exhibited the opposing response within the distal colon, which showed an increase of Proteobacteria (mean 49%) and a decrease of Bacteroidetes (mean 22%) and Firmicutes (mean 27%) in comparison to the proximal region of the colon (Fig. 1B).

Phylogenetic classification of the mucosa-attached microbiota across the dataset identified 15 major bacterial families encompassing 6 bacterial classes: *Actinobacteria*, *Bacteroidia*, *Bacilli*, *Clostridia*, *Epsilonproteobacteria* and *Gammaproteobacteria*. In the small intestine (duodenum, jejunum, ileum) *Epsilon*- and *Gammaproteobacteria* were the dominant classes, comprised mainly of three families, *Campylobacteraceae*, *Helicobacteraceae* and *Enterobacteraceae*, accounting for average levels of 40%, 23% and 10% of total bacteria respectively (Fig. 1C). In the large intestine (caecum, proximal colon, distal colon) however, the abundance of *Bacteroidia* and *Clostridia* increased with *Prevotellaceae*, *Lachnospiraceae*, *Ruminococcaceae* and *Veillonellaceae* all becoming major constituents of the mucosa-associated microbiota (mean abundance 19%, 6%, 11% and 9% of total respectively) (Fig. 1C).

In general, these predominant families were represented by one or two very highly abundant OTUs, which usually accounted for the majority of that particular family within the mucosa. The most dominant OTU throughout the entire length of the intestinal tract (designated OTU3063) showed 100% sequence identity to *Campylobacter coli*. In both the duodenum and jejunum, this *Campylobacter*-OTU accounted for a mean abundance of over 50% of the entire mucosal microbiota, and was the most abundant single OTU in all gut regions except ileum and caecum (Fig. 2A).

The majority of intestinal regions also harboured a consistently high level of *Helicobacteraceae*, comprised of a small number of OTUs whose abundance was correlated with specific intestinal

regions. One of these OTUs (OTU2377), with 100% sequence identity to *Helicobacter rappini*, represented a substantial proportion of the mucosal microbiome within the duodenum and jejunum (mean abundance of 24% in both regions) (Fig. 2B), whilst an unclassified *Helicobacter*-OTU (OTU1319) was the most abundant OTU within the caecum (mean 18% of total) (Fig. 2C).

Similarly, the majority of *Prevotellaceae* abundance was due to a single OTU (OTU3059), showing 100% sequence identity to *Prevotella copri* (Fig. 2D), with the abundance of *Lachnospiraceae*, *Ruminococcaceae* and *Veillonellaceae* also due mainly to two or three individual OTUs.

Although many microbial groups exhibited a consistent presence throughout the length of the pig intestinal tract, the overall composition of the mucosa-associated microbiome was found to be significantly associated with gut location (ANOSIM R: 0.32, $P < 0.001$, weighted Unifrac). Not surprisingly, the strongest correlation between microbial community membership and gut location was observed between small and large intestinal bacterial populations (ANOSIM R: 0.43, $P < 0.001$, weighted Unifrac). PCoA results illustrate this clearly, revealing a distinct separation of bacterial community structure when grouped by small and large intestine (Fig. 3A). The mucosa of the large intestine also harboured a significantly higher level of microbial diversity in comparison to the small intestine ($P < 0.05$, Shannon diversity index). This can also be seen by the number of distinct OTUs observed in each region; the mucosa of the small intestine of each pig containing an average of 42 OTUs, with the mucosa of the large intestine having an average of 79 OTUs (minimum 0.1% of total) ($P < 0.001$). The mean number of OTUs representing at least 1% of the total mucosa-associated microbiota was also increased in the large intestine (mean of 16) compared to small (mean of 9) ($P < 0.01$).

In total, over 150 phylotypes exhibited significant differential regional abundances ($P < 0.05$) between the mucosa-associated microbiome of the small and large intestine. The previously mentioned *H. rappini*-OTU (OTU2377), which accounted for a mean abundance of 18% within the

small intestine microbiome, was present at significantly lower levels in the large intestine (mean 4%) ($P < 0.05$) (Fig. 2B). In contrast, *Helicobacter*-OTU1319 was present at significantly lower levels in the small intestine (mean 0.1%) compared to the mucosa of the caecum (mean 18%) ($P < 0.05$) (Fig. 2C). One other notable difference, within the *Proteobacteria*, between the mucosal microbiota of the small and large intestine was the 15-fold reduction of *Escherichia coli*-OTU2459 from a mean of 6% of the total mucosa-associated microbiota in the ileum down to 0.4% in the large intestine ($P < 0.05$) (Fig. 2E).

Within the large intestine, there was a significant mucosal enrichment of OTUs classified as fibre degraders and/or short chain fatty acid (SCFA) producers compared to the small intestine, specifically within the *Prevotellaceae* (5.1-fold), *Lachnospiraceae* (3.5-fold), *Ruminococcaceae* (2.8-fold) and *Veillonellaceae* (3.4-fold) families ($P < 0.05$). This is consistent with the role of large intestinal bacterial populations in fibre fermentation and SCFA production. The *Prevotellaceae* family was particularly enriched within the large intestine, with the previously mentioned *P. copri*-OTU3059 increasing from a mean abundance of 2% to almost 8% of total from small to large intestine ($P < 0.01$) (Fig. 2D). Within the *Lachnospiraceae*, *Ruminococcaceae* and *Veillonellaceae* families, OTUs classified as *Roseburia* (OTU3055), *Faecalibacterium* (OTU1672) and *Megasphaera* (OTU12) also demonstrated similar fold increases in the large compared to the small intestine ($P < 0.01$) (Fig. 2F-H).

Notably, determination of total 16SrRNA gene copy number, by quantitative PCR, showed that the density of mucosa associated bacteria increased aborally in the intestine, with significantly higher copy numbers in the proximal and distal colon compared to duodenum and jejunum ($P<0.05$) (Fig. 4).

Comparison of the mucosa-associated and luminal microbiota of pig caecum

We determined potential differences in microbial populations between those residing within the mucosa compared to those in the lumen. To this end, 16S rRNA genes amplified from caecal contents and mucosal scrapings of pigs were sequenced. Interestingly, bacterial composition

differed significantly between the two sample types (ANOSIM R: 0.66, $P < 0.001$, Weighted Unifrac,). As shown in Fig. 3B there is a distinct separation of lumenal content bacteria from those associated with the outer mucosal layer. Furthermore, lumenal content harboured a significantly more diverse microbiota than the mucosa-associated population ($P < 0.05$, Shannon diversity index).

ANOSIM and PCoA analyses demonstrated that there were substantial differences between the microbiota of the caecal lumen and mucosa, with 57 OTUs identified as differentially abundant between the two locations ($P < 0.05$). Composition of the caecal mucosa-associated microbiome was characterised by a dominance of *Proteobacteria*, namely *Campylobacteraceae* and *Helicobacteraceae*, and lack of *Bacteroidetes* and *Firmicutes*, in comparison to the lumenal content microbiota (Fig. 5).

Helicobacteraceae accounted for 32% of the total microbial community within the mucosa but less than 0.1% in the lumen ($P < 0.05$) (Fig. 5). This was primarily attributable to the significant mucosal enrichment of the dominant large intestinal *Helicobacter*-OTU1319, which accounted for almost one fifth of the caecal mucosa-associated microbiota (mean 18%), but was present at negligible levels within the lumen (<0.1%) ($P < 0.01$) (Fig. 6A). Levels of *C. coli*-OTU3063 were also significantly higher within the caecal mucosa compared to the lumenal contents, increasing from a mean abundance of 0.6% in the lumen to over 15% within the mucosal layer ($P < 0.05$) (Fig. 6B).

Members of the *Prevotellaceae* were substantially reduced within mucosa-associated communities in comparison to those residing in the lumen. Altogether 98 *Prevotella*-OTUs were significantly lower in abundance between the mucosa and the lumen of the caecum, with one particular OTU (OTU3059), most closely matching *P. copri*, reducing from a mean abundance of 17% of total in the lumen to 6% within the mucosal layer ($P < 0.05$) (Fig. 6C).

A number of other OTUs were also found at a lower abundance in the caecal mucosa compared to the lumen, including those assigned as *Roseburia* (within the *Lachnospiraceae* family) and *Megasphaera* (within the *Veillonellaceae*) ($P < 0.05$).

The impact of dietary supplementation with the sweetener SUCRAM on mucosa-associated microbial communities

We have previously investigated the effect of dietary supplementation with the artificial sweetener SUCRAM upon the microbiota within the lumenal contents of the pig caecum. This sweetener is now routinely included in the diet of weaning piglets on a commercial basis. Our results demonstrated that SUCRAM profoundly influences the composition and activity of the lumenal caecal microbiome (Daly *et al*., 2015). In this paper, we sought to determine if this sweetener may also affect the mucosa-associated microbiota of the intestine.

Indeed, the addition of SUCRAM to the piglets' diet had a significant impact on the composition of the mucosa-associated microbiota throughout the entire length of the intestinal tract (Fig. 7) ($P < 0.05$). In the small intestine, the relative abundance of 76 mucosa-associated OTUs were significantly different between pigs weaned to the basal diet (BD) compared to those weaned to the SUCRAM-supplemented diet (BD+S) ($P < 0.05$), whilst a total of 81 were significantly altered in the large intestine ($P < 0.05$).

There were pronounced differences in composition of the mucosa-associated microbiota of the duodenum, jejunum and ileum in response to consumption of BD+S diet. The major effect was a dramatic shift in the population abundance of the two predominant families within these intestinal regions, *Campylobacteraceae* and *Helicobacteraceae* (Fig. 7). Relative abundance levels of total *Campylobacteraceae* were dramatically lower in the small intestine of BD+S pigs (0.3%) compared to BD pigs (40%) ($P < 0.01$) due to the significant depletion of the predominant *C. coli*-OTU3063 (Fig. 8A). Although relative abundance of this OTU was significantly reduced within the small intestine overall ($P < 0.05$), the response to dietary supplementation with SUCRAM was strongest in the duodenal mucosa, where its mean relative abundance was reduced > 200-fold compared to BD pigs

This article has been accepted for publication and undergone full peer review but has not been through the copyediting, typesetting, pagination and proofreading process which may lead to differences between this version and the Version of Record. Please cite this article as an 'Accepted Article', doi: 10.1111/1462-2920.13361

(from 57% to 0.2%; $P < 0.05$) (Fig. 8A). This OTU was also maintained at greatly reduced levels throughout the large intestine of BD+S-fed pigs (from 24% to 6% of total; $P < 0.05$) (Fig. 8A).

Quantitative analysis of total 16SrRNA gene copies in the duodenum and jejunum of BD+S pigs showed no significant differences in comparison to BD pigs (data not shown), equating to a comparative reduction in 16S rRNA gene copy number for *C. coli*-OTU3063 of over 99% and 96% in the duodenum and jejunum of BD+S pigs respectively ($P<0.001$ for both) (Fig. 9).

There was an opposite profile for *Helicobacteraceae* in the small intestinal mucosa of pigs weaned to the BD+S diet, increasing significantly from a mean abundance of 23% in BD pigs to 60% in BD+S pigs ($P < 0.01$) (Fig. 7). The difference in total *Helicobacteraceae* abundance was determined by the significant enrichment of *H. rappini*-OTU2377 (Fig. 8B). In response to dietary supplementation with SUCRAM, this individual OTU accounted for 50% of the total mucosal microbiota, thereby representing the most abundant OTU in the entire small intestinal mucosa of BD+S pigs. However, this response was limited to the small intestinal tract, with no significant sweetener-induced differences in Helicobacteraceae abundance in the large intestine (Fig. 7).

Within the large intestine, the effects of SUCRAM supplementation were distinct from those observed in the small intestine and mainly involved specific OTUs within the *Bacteroidetes* and *Firmicutes* phyla (Fig. 7). In particular, there was a 16-fold higher abundance of one particular *Lactobacillus*-OTU (OTU2018), related to *Lactobacillus gasseri*, with a mean abundance of 0.3% in the mucosa of the large intestine of BD pigs compared to 5% in BD+S pigs ($P < 0.05$) (Fig. 8C).

Discussion

The gut contains a diverse microbiota with a large potential to influence host health. The mucosa-associated microbiome, residing within the outer mucus layer holds a notable position in the intestine. They play an important role in determining bacterial-triggered host immune activation and gut brain communication (Bienenstock *et al*., 2015; Mayer et al., 2015; Min and Rhee, 2015; Thaiss et al., 2016).

Thus, characterisation of this microbial community is highly informative to our understanding of host-microbiome interactions, in both health and disease.

In this study, using next-generation Illumina sequencing, we show that the composition of the pig mucosa-associated microbiota is largely influenced by gut location, with distinct separation between small and large intestinal populations. We demonstrate that the small intestine is dominated by *Proteobacteria*, while *Bacteroidetes* and *Firmicutes* are the most prevalent phyla in the large intestine.

There are several factors that may be responsible for this shift in bacterial community profile. Physicochemical conditions and substrate availability differ aborally through the intestinal tract, creating a range of divergent microenvironments that can promote distinct microbial populations (Stearns *et al*., 2011; Zhao *et al*., 2015). Proximity to the mucosal layer exposes the mucosa-associated microbiome to a host-derived oxygen source (Marteyn *et al*., 2010; Albenberg *et al*., 2014), promoting the growth of oxygen-tolerant populations such as members of the Proteobacteria. However, mucus thickness and viscosity increases longitudinally along the length of the intestinal tract (Atuma *et al*., 2001; Johansson *et al*., 2008), creating a diffusion barrier and reducing oxygen tension in the mucosa of the large intestine (Moran, 2014). This condition promotes the enrichment of anaerobic oxygen-sensitive communities such as Bacteroidetes and Firmicutes.

This article has been accepted for publication and undergone full peer review but has not been through the copyediting, typesetting, pagination and proofreading process which may lead to differences between this version and the Version of Record. Please cite this article as an 'Accepted Article', doi: 10.1111/1462-2920.13361

Wiley-Blackwell and Society for Applied Microbiology

Many groups within the Bacteroidetes and Firmicutes proliferate by hydrolysing dietary fibre and complex carbohydrates. The findings that *Prevotella, Ruminococcaceae, Lachnospiraceae* and *Veillonellaceae* are highly abundant in the mucosa of the caecum and proximal colon of pigs but decline in the distal colon, where amounts of complex carbohydrates become limiting, suggest that substrate availability is also a major factor for dynamics of mucosa-associated populations.

One interesting aspect of our investigations is the predominance of only a small number of distinct OTUs. We have identified 382 OTUs resident in the pig intestinal tract mucosa, with each individual pig harbouring an average of 42 OTUs in the small and 79 OTUs in the large intestine (> 0.1% relative abundance). However, the contribution of just the 10 most abundant OTUs, within each intestinal region, encompasses 57%-88% of the total microbiota in the small and between 29%-66% in the large intestine. Furthermore 4 OTUs that were common to the top 10 most abundant in both regions (OTU3063, OTU2377, OTU3059 and OTU1672; Fig. 2) accounted for between 24%-74% of total in the small intestine and between 14%-52% in the large intestine. These data raise the possibility of the existence of a core mucosa-associated microbiome in the pig intestine, as has been recently postulated for the gut microbiota of humans and other species (Tap *et al*., 2009; Turnbaugh *et al*., 2009; Roeselers *et al*., 2011; O'Donnell *et al*., 2013; Wong *et al*., 2013; Dill-McFarland *et al*., 2014).

Differences in the composition of the mucosa-associated microbiota to those residing within the lumen have been identified in a number of studies (Zoetendal *et al*., 2002; Nava *et al*., 2011; Galley *et al*., 2014) and the results shown here support these observations. Oxygen diffusion from the host capillary network creates a microenvironment within the mucosa that can support oxygen-tolerant microaerophilic species (Albenberg *et al*., 2014). Indeed, a recent study revealed that mucosal bacteria consume the majority of available oxygen, limiting its diffusion into the lumen (Albenberg *et al*., 2014). Here, we observed that the mucosal layer of the caecum is enriched with the microaerophilic families *Campylobacteraceae* and *Helicobacteraceae* (Kelly, 2001), in comparison to

the caecal lumen where they are almost completely absent. Both these groups are adept at survival within the outer mucus layer, owing to their microaerophilic metabolism, effective flagella-propelled motility in a viscous environment (Szymanski *et al*., 1995; Kelly, 2001; Beeby, 2015) and mucin-colonising abilities (Mahdavi *et al*., 2002; Naughton *et al*., 2013).

Within the lumen of the caecum, we observed a significant enrichment of the obligate anaerobe family *Prevotellaceae*, in comparison to the mucosa. The ability of many *Prevotellaceae* to degrade complex carbohydrates (Shah and Collins, 1990; Hayashi *et al*., 2007), and their intolerance to oxygen, are likely reasons for their high abundance in the lumen. Moreover, other carbohydrate-fermenting species such as *Faecalibacterium* and *Roseburia* were also found at significantly higher levels in the lumen compared to the mucosa. Interestingly, although members of the *Prevotellaceae* were more abundant in the lumen, notable levels were also observed amongst the mucosal microbiome, where they comprised approximately one fifth of the entire community. Certain *Prevotellaceae* have well established mucin-degrading capabilities (Wright *et al*., 2000). Therefore the mucosal layer provides an additional nutrient source, and although the aerobic microenvironment of the mucosa may be expected to restrict the growth of *Prevotellaceae*, strain-level variation in oxygen tolerance (Silva *et al*., 2003) may help to explain its significant presence in the mucosa-associated microbiome (Looft *et al*., 2014; Mann *et al*., 2014; Yasuda *et al*., 2015). These data suggest that both oxygen tension and substrate availability play major roles in shaping the composition of, and defining differences between, the mucosa-associated and lumenal microbiomes.

The supplementation of the diet with the artificial sweetener SUCRAM had a marked effect on the composition of the mucosa-associated microbiota along the entire length of the intestinal tract, emphasising the conclusion made by Daly *et al*. (2015) that supplementation of the diet with SUCRAM has a major influence on bacterial community structure in the pig intestine. Indeed, the significant increase in probiotic *Lactobacillaceae* population abundance reported by Daly *et al*. (2015)

This article has been accepted for publication and undergone full peer review but has not been through the copyediting, typesetting, pagination and proofreading process which may lead to differences between this version and the Version of Record. Please cite this article as an 'Accepted Article', doi: 10.1111/1462-2920.13361

Wiley-Blackwell and Society for Applied Microbiology

in the caecal contents of pigs fed the BD+S diet compared to the BD diet, was also observed here both within the caecal lumen and mucosa-associated microbiota. Our investigation into the underlying mechanisms (Daly *et al*., 2015) demonstrated that NHDC (a sweetener component of SUCRAM) significantly reduces lag phase of growth of *Lactobacillus* and enhances expression of specific sugar transporters, independent of NHDC metabolism. Our experimental evidence suggested that sensing of NHDC by a bacterial plasma membrane receptor underlies NHDC-induced proliferation of *Lactobacillus* (Daly *et al*. 2015).

In this study, one of the more notable and pertinent effects of dietary supplementation with SUCRAM is the dramatic reduction in abundance of the *Campylobacteraceae*, and in particular *Campylobacter coli* (OTU3063), not only in terms of relative, but also absolute population abundance.

Campylobacter coli is a common commensal inhabitant of the pig gastrointestinal tract (Harvey *et al*., 1999), with 50% - 100% prevalence and excretion levels varying from 10^2 to 10^7 CFU g^{-1} faeces (Alter *et al*., 2005; Jensen *et al*., 2005). While it does not normally cause enteric disease in pigs (Aguilar *et al*., 2014), a recent study (Burrough *et al*. 2013) reported that in up to 15% of pig diarrhoeal disease cases, *Campylobacter* was the sole infectious agent.

Perhaps of more importance from a human perspective is that campylobacteriosis is one of the most frequently reported zoonotic bacterial infections, with estimates ranging from approximately 800,000 to 2 million people infected with *Campylobacter* annually in the United States alone (Samuel *et al*., 2004; Scallen *et al*., 2011). Although *C. jejuni* is considered the principle *Campylobacter* species causing infection in humans (Allos, 2001), *C. coli* is now being regarded as one of the major causative agents of food-borne enteritis worldwide, accounting for up to 10% of human campylobacteriosis cases (Gillespie *et al*., 2002; Tam *et al*., 2003). One study in particular identified

almost 20% of *Campylobacter* cultures isolated from human patients as being *C. coli* (Gurtler *et al*., 2005).

Furthermore, a recent study has reported up to 10% incidence of *Campylobacter* contamination of retail pork meat (Korsak *et al*., 2015); most likely occurring through faecal contact (Boysen and Rosenquist, 2009). Considering that many strains of *Campylobacter* have become multi-drug resistant (Bywater *et al*., 2004; Englen *et al*., 2005; Bernal *et al*., 2016; Wang *et al*., 2016), it is notable that reduction of pig intestinal *Campylobacter* load can be achieved through the simple supplementation of the diet with SUCRAM, minimising meat contamination. This has important health implications relating to food safety and avoidance of disease risk worldwide (Niederer *et al*., 2012). Moreover, the findings demonstrate that even small dietary changes could have profound effects on the mucosa-associated microbiota, which opens up the possibility that new therapeutic strategies can be developed for bacterial-associated gut disorders.

Experimental Procedures

Animals and collection of samples

Male and female suckling Gloucestershire Old Spot piglets aged 28 days were placed in pairs and housed in standard pens (1.5-m^2, 12 h light/dark cycle, 26 °C). Two groups, each consisting of 8 animals, were weaned to and maintained on the following isoenergetic, 16.76 kJ / g, swine diets (Target Feeds Ltd, Shropshire, UK) for two weeks: (Group 1) a wheat- and soya-based basal diet (BD) containing 42% (w/w) digestible carbohydrates, or (Group 2) the same basal diet but supplemented with 0.015% (w/w) SUCRAM (BD+S) (For composition of diets see Daly *et al*., 2015). All animals had free access to food and water at all times with each group consuming the same amount of feed (BD: 405.7 g / day ± 139.6; BD+S: 401.5 g / day ± 204.3). Animals remained healthy throughout the course of feeding trial, and had no signs of enteric or metabolic disturbances. After two weeks, piglets were killed with an intravenous injection of pentobarbitone (200 mg/ml Pentoject; AnimalCare Ltd, Yorkshire, UK) to the cranial vena cava (according to UK Home Office Schedule 1 regulations). Immediately post-mortem, mucosal scrapings from duodenum, jejunum, ileum, caecum, proximal colon and distal colon were removed, washed in ice-cold 0.9% saline, wrapped in aluminium foil and frozen in liquid nitrogen. All samples were subsequently stored at −80°C. National/institutional guidelines for the care and use of animals were followed, and all experiments were approved by the University of Liverpool Ethics Committee.

Extraction of bacterial DNA from mucosal scrapings

Nucleic acid was extracted from mucosal scrapings using the method described by Daly & Shirazi-Beechey (2003). Approximately 0.5 g aliquots of frozen samples were transferred to screw-cap tubes containing SDS, Tris-buffered phenol (pH 8.0) (Sigma-Aldrich Co. Ltd, Dorset, UK) and sterile acid-

This article has been accepted for publication and undergone full peer review but has not been through the copyediting, typesetting, pagination and proofreading process which may lead to differences between this version and the Version of Record. Please cite this article as an 'Accepted Article', doi: 10.1111/1462-2920.13361

washed glass beads. Samples were immediately homogenised using a mini beadbeater (Biospec Corp., Stratech Scientific, Sussex, UK). The aqueous supernatant was then extracted with phenol-chloroform-isoamylalcohol and treated with DNase-free RNase A to remove any potential contaminating RNA. Total DNA was precipitated by the addition of sodium acetate and isopropanol. DNA was resuspended in sterile Tris buffer and purified using the QIAquick PCR purification kit (Qiagen, Sussex, UK) before storage at −80°C. Purified DNA was quantified using PicoGreen Assay (Life Technologies Ltd, Paisley, UK) and integrity was assessed by agarose gel electrophoresis. We have observed that rapid freezing of samples in liquid nitrogen, followed by homogenisation in a buffer containing phenol, is an effective method for inactivating nuclease activity (Daly & Shirazi-Beechey, 2003). This approach also avoids repeated freeze-thawing of samples that may be deleterious to the efficient isolation of DNA from gram negative microbes.

PCR amplification of bacterial 16S rRNA genes and Illumina MiSeq sequencing

Purified genomic DNA extracted from mucosal scrapings was used as template for PCR amplification of the hypervariable V4-region of bacterial 16S rRNA genes using custom primers designed by Caporaso *et al*. (2012), which comprised the universal forward and reverse bacterial primers 515f and 806r, and the required Illumina flowcell adaptor sequences (Caporaso *et al*., 2012). The reverse primer also contained a unique 12 base Golay barcode to allow multiplexing of numerous samples (Caporaso *et al*., 2012). To reduce PCR-associated bias and to increase DNA yield, the products of several amplification reactions for each sample were pooled. Each reaction mix contained 0.5 U of Q5 Hot Start High-Fidelity DNA Polymerase (New England Biolabs, Suffolk, UK), 1.25 µl of each primer (10 µM), 0.5 µl dNTPs (10 mM), 5 µl of 5X Q5 Reaction Buffer (New England Biolabs) and 20 ng genomic DNA in a final volume of 25 µl. PCR amplification was carried out using the following parameters: initial denaturation at 98°C for 30 s, 26 or 18 cycles (small and large intestine

This article has been accepted for publication and undergone full peer review but has not been through the copyediting, typesetting, pagination and proofreading process which may lead to differences between this version and the Version of Record. Please cite this article as an 'Accepted Article', doi: 10.1111/1462-2920.13361

Wiley-Blackwell and Society for Applied Microbiology

respectively) of denaturation at 98°C for 10 s, annealing at 55°C for 20 s and elongation at 72°C for 15 s, followed by a final elongation step at 72°C for 2 min. Samples were then combined with 5 µl loading buffer and subjected to electrophoresis at 100 V in 1 x TAE buffer. Amplified product of the target length was visualised, excised and purified using the QIAquick Gel Extraction kit according to manufacturer's protocol (Qiagen). No-template controls were also generated for all samples. Samples were then quantified in duplicate using the Quant-it PicoGreen dsDNA kit (Life Technologies Ltd). Quantified samples were finally combined in equimolar amounts and sequenced on the Illumina MiSeq sequencing platform at the Centre for Genomic Research (CGR) next-generation sequencing facility at the University of Liverpool, UK.

Read filtering and paired-end assembly

Raw sequencing reads underwent a strict filtering pipeline to remove low-quality reads. A standard read-filtering pipeline on all sequenced datasets was employed. This comprises: i) the removal of Illumina adaptor sequences using CutAdapt (version 1.2.1) (Martin, 2011); ii) the trimming of low-quality bases using Sickle (https://github.com/najoshi/sickle) (version 1.2), utilising a sliding window of a defined size to remove read segments which do not have a minimum phred quality value of 20, and iii) the removal of any trimmed reads below 10 bp in length. High-quality paired-end reads were then assembled into overlapping sequences using the assembly software FLASH (Magoc and Salzberg, 2011) based on the following parameters: minimum overlap: 25, maximum overlap: 250, maximum ratio between number of mismatches and overlap length: 0.25. Only assembled sequences above 200 bp in length were retained. Assembled sequences were then filtered for any contaminating phiX sequence that may have been carried over from the sequencing process using BMtagger (Rotmistrovsky and Agarwala, 2011) and the NCBI reference sequence for *Enterobacteria* phage phiX174 (NCBI accession NC001422).

This article has been accepted for publication and undergone full peer review but has not been through the copyediting, typesetting, pagination and proofreading process which may lead to differences between this version and the Version of Record. Please cite this article as an 'Accepted Article', doi: 10.1111/1462-2920.13361

Microbial profiling analysis

Unless otherwise stated, all analysis described in this section was carried out using the software package Quantitative Insights into Microbial Ecology (QIIME v1.8.0) (Caporaso *et al*., 2010a). Following quality filtering and assembly, a total of 43,252,569 reads were generated for 105 samples, with an average (± SD) of 411,929 ± 109,438 reads per sample. Sequences were clustered into operational taxonomic units (OTUs) at 97% similarity using the USEARCH algorithm (Edgar, 2010) with a minimum cluster size of 10. Chimeric sequences were filtered using both de-novo (UCHIME) (Edgar *et al*., 2011) and reference based approaches. The most abundant sequence was selected from each OTU cluster and assigned taxonomic classification using the Ribosomal Database Project (RDP) (Cole *et al*., 2009) classifier tool with the most recent release of the Greengenes database (13.8) (DeSantis *et al*., 2006), using a confidence cut-off of 0.8. PyNAST (Caporaso *et al*., 2010b) was then utilised to generate alignments for all representative sequences, which were subsequently filtered and used to generate a phylogeny using the FastTree approach (Price *et al*., 2009). Microbial richness and diversity (alpha diversity) was calculated using the Chao1 non-parametric richness estimator (Chao, 1984) and Shannon diversity index (Shannon and Weaver, 1971) metrics using a rarefaction depth of 179,000 reads. To determine the degree of similarity between samples (beta-diversity), both weighted and unweighted Unifrac distance matrices were calculated for all pair-wise sample comparisons, and used to generate principal co-ordinates analyses (PCoA) plots and Unweighted Pair Group Method with Arithmetic mean (UPGMA) dendrograms.

Statistical analysis

To test for differences in microbial diversity/richness between intestinal locations and different diets, non-parametric two-sample t tests were used with Monte Carlo permutations to calculate the p-

This article has been accepted for publication and undergone full peer review but has not been through the copyediting, typesetting, pagination and proofreading process which may lead to differences between this version and the Version of Record. Please cite this article as an 'Accepted Article', doi: 10.1111/1462-2920.13361

Wiley-Blackwell and Society for Applied Microbiology

value (999 permutations). The significance and strength of a range of sample groupings (i.e. diet, intestinal region, individual) was determined by comparing beta-diversity matrices of weighted Unifrac and unweighted Unifrac distances using a range of non-parametric tests including ADONIS and ANOSIM (Anderson *et al*., 2006). The ADONIS test also revealed the amount of sample variance (effect size) attributable to each grouping category. Differentially abundant OTUs were identified using the statistical software Metastats (White *et al*., 2009), which applies non-parametric t tests using 1000 permutations and generates a false discovery rate (FDR)-corrected p-value (q-value) which corrects for multiple comparisons (Benjamini and Hochberg, 1995). Features were considered significant if both *P* values and *q* values were less than 0.05. Prior to differential abundance testing data was rarefied and all OTUs and taxonomic groups below 0.05% relative abundance were removed.

Plots were generated using the software packages R, version 3.1.1 (Grimonprez *et al*., 2014), QIIME (versions 1.8 and 1.9) (Caporaso *et al*., 2010a) and Phyloseq (McMurdie and Holmes, 2013).

Quantitative real-time PCR analysis of microbial abundance

Quantification of 16S rRNA gene copy number in DNA extracted from pig mucosal scrapings was determined by qPCR using a Rotorgene 3000 (Qiagen) and SYBR Green JumpStart Taq ReadyMix for qPCR (Sigma Aldrich Co. Ltd). Total 16S rRNA gene copy number was determined in each sample, as a measurement of total bacterial numbers (Barman *et al*., 2008), by amplification of bacterial DNA with universal 16S rRNA gene primers, in comparison to standard curves constructed from a reference plasmid containing the 16S rRNA gene from *Lactobacillus amylovorus* (Daly *et al*., 2015). PCR cycling was performed as follows: initial denaturation at 95^{o}C for 2 min followed by 40 cycles of 95^{o}C for 13 s, 63^{o}C for 15 s, 72^{o}C for 30 s. Assays were performed in triplicate and 16S rRNA gene copy number was calculated using RG-3000 quantification software.

This article has been accepted for publication and undergone full peer review but has not been through the copyediting, typesetting, pagination and proofreading process which may lead to differences between this version and the Version of Record. Please cite this article as an 'Accepted Article', doi: 10.1111/1462-2920.13361

Acknowledgements

This study was supported by Pancosma SA, Geneva, Switzerland.

JK, AWM, SR and SPS-B designed the research; JK, AWM and SR performed sequencing; JK performed bioinformatics analyses of sequencing data; KD performed quantitative PCR analyses; DB provided reagents and nutritional advice; KD, JK and SPS-B wrote different parts of the paper, with SPSP revising the final draft.

The authors have no conflicts of interest to declare. Pancosma had no involvement in design, implementation or interpretation of data presented in this paper.

References

Aguilar C, Jiménez-Marín Á, Martins RP, Garrido JJ (2014). Interaction between *Campylobacter* and intestinal epithelial cells leads to a different proinflammatory response in human and porcine host. *Vet Immunol Immunopathol* **162**: 14-23.

Ahmed S, Macfarlane GT, Fite A, McBain AJ, Gilbert P, Macfarlane S (2007). Mucosa-associated bacterial diversity in relation to human terminal ileum and colonic biopsy samples. *Appl Environ Microbiol* **73**: 7435-7442.

Albenberg L, Esipova TV, Judge CP, Bittinger K, Chen J, Laughlin A (2014). Correlation between intraluminal oxygen gradient and radial partitioning of intestinal microbiota. *Gastroenterology* **147**: 1055-1063.

Allos BM (2001). *Campylobacter jejuni* infections: update on emerging issues and trends. *Clin Infect Dis* **32**: 1201-1206.

Alter T, Gaull F, Kasimir S, Gürtler M, Mielke H, Linnebur M *et al*. (2014). Prevalences and transmission routes of *Campylobacter* spp. strains within multiple pig farms. *Vet Microbiol* **108**: 251-261.

Anderson MJ, Ellingsen KE, McArdle BH (2006). Multivariate dispersion as a measure of beta diversity. *Ecol Lett* **9**: 683-693.

Atuma C, Strugala V, Allen A, Holm L (2001). The adherent gastrointestinal mucus gel layer: thickness and physical state *in vivo*. *Am J Physiol Gastrointest Liver Physiol* **280**: G922-G929.

Barman M, Unold D, Shifley K, Amir E, Hung K, Bos N *et al*. (2008). Enteric salmonellosis disrupts the microbial ecology of the murine gastrointestinal tract. *Infect Immun* **76**: 907-915.

Beeby M (2015). Motility in the epsilon-proteobacteria. *Curr Opin Microbiol* **28**: 115-121.

Benjamini Y, Hochberg Y (1995). Controlling the false discovery rate: a practical and powerful approach to multiple testing. *J R Statist Soc B* **57**: 289–300.

Bernal JF, Donado-Godoy P, Valencia MF, León M, Gómez Y, Rodríguez F *et al*. (2016). Whole-genome sequences of two *Campylobacter coli* isolates from the antimicrobial resistance monitoring program in Colombia. *Genome Announc* **4**: e00131-16.

Bevins CL, Salzman NH (2011). Paneth cells, antimicrobial peptides and maintenance of intestinal homeostasis. *Nat Rev Microbiol* **9**: 356-368.

Bienenstock J, Kunze W, Forsythe P (2015). Microbiota and the gut-brain axis. *Nutr Rev* **73** (Suppl 1): 28-31.

Bik EM, Eckburg PB, Gill SR, Nelson KE, Purdom EA, Francois F *et al*. (2006). Molecular analysis of the bacterial microbiota in the human stomach. *Proc Natl Acad Sci USA* **103**: 732-737.

Boysen L, Rosenquist H (2009). Reduction of thermotolerant *Campylobacter* species on broiler carcasses following physical decontamination at slaughter. *J Food Prot* **72**: 497-502.

Burrough E, Terhorst S, Sahin O, Zhang Q (2013). Prevalence of *Campylobacter* spp. relative to other enteric pathogens in grow-finish pigs with diarrhea. *Anaerobe* **22**: 111-114.

Bywater R, Deluyker H, Deroover E, de Jong A, Marion H, McConville M *et al*. (2004). A European survey of antimicrobial susceptibility among zoonotic and commensal bacteria isolated from food-producing animals. *J Antimicrob Chemother* **54**: 744-754.

Caporaso JG, Kuczynski J, Stombaugh J, Bittinger K, Bushman FD, Costello EK *et al*. (2010a). QIIME allows analysis of high-throughput community sequencing data. *Nat Methods* **7**: 335-336.

Caporaso JG, Bittinger K, Bushman FD, DeSantis TZ, Andersen GL, Knight R (2010b). PyNAST: a flexible tool for aligning sequences to a template alignment. *Bioinformatics* **26**: 266-267.

Caporaso JG, Lauber CL, Walters WA, Berg-Lyons D, Huntley J, Fierer N *et al*. (2012). Ultra-high-throughput microbial community analysis on the Illumina HiSeq and MiSeq platforms. *ISME J* **6**: 1621-1624.

Chao A (1984). Nonparametric estimation of the number of classes in a population. *Scand J Statist* **11**: 265-270.

Cole JR, Wang Q, Cardenas E, Fish J, Chai B, Farris RJ *et al*. (2009). The Ribosomal Database Project: improved alignments and new tools for rRNA analysis. *Nucleic Acids Res* **37**: D141-D145.

Daly K, Shirazi-Beechey SP (2003). Design and evaluation of group-specific oligonucleotide probes for quantitative analysis of intestinal ecosystems: their application to assessment of equine colonic microflora. *FEMS Microbiol Ecol* **44**: 243-252.

Daly K, Darby AC, Hall N, Wilkinson MC, Pongchaikul P, Bravo D *et al*. (2015). Bacterial sensing underlies artificial sweetener-induced growth of gut *Lactobacillus*. *Environ Microbiol* **18**: 2159-2171.

Daly K, Darby AC, Shirazi-Beechey SP (2016). Low calorie sweeteners and gut microbiota. *Physiol Behav* **164** (Pt B): 494-500.

DeSantis TZ, Hugenholtz P, Larsen N, Rojas M, Brodie EL, Keller K *et al*. (2006). Greengenes, a chimera-checked 16S rRNA gene database and workbench compatible with ARB. *Appl Environ Microbiol* **72**: 5069-5072.

Dill-McFarland KA, Neil KL, Zeng A, Sprenger RJ, Kurtz CC, Suen G *et al*. (2014). Hibernation alters the diversity and composition of mucosa-associated bacteria while enhancing antimicrobial defence in the gut of 13-lined ground squirrels. *Mol Ecol* **23**: 4658-4669.

Edgar RC (2010). Search and clustering orders of magnitude faster than BLAST. *Bioinformatics* **26**: 2460-2461.

Edgar RC, Haas BJ, Clemente JC, Quince C, Knight R (2011). UCHIME improves sensitivity and speed of chimera detection. *Bioinformatics* **27**: 2194-2200.

Englen MD, Fedorka-Cray PJ, Ladely SR, Dargatz DA (2005). Antimicrobial resistance patterns of *Campylobacter* from feedlot cattle*. *J Appl Microbiol* **99**: 285-291.

Galley JD, Yu Z, Kumar P, Dowd SE, Lyte M, Bailey MT (2014). The structures of the colonic mucosa-associated and luminal microbial communities are distinct and differentially affected by a prolonged murine stressor. *Gut Microbes* **5**: 748-760.

Gillespie IA, O'Brien SJ, Frost JA, Adak GK, Horby P, Swan AV *et al*. (2002). A case-case comparison of *Campylobacter coli* and *Campylobacter jejuni* infection: a tool for generating hypotheses. *Emerg Infect Dis* **8**: 937-942.

Grimonprez Q, Celisse A, Blanck S, Cheok M, Figeac M, Marot G (2014). MPAgenomics: an R package for multi-patient analysis of genomic markers. *BMC Bioinformatics* **15**: 394.

Gürtler M, Alter T, Kasimir S, Fehlhaber K (2005). The importance of *Campylobacter coli* in human campylobacteriosis: prevalence and genetic characterization. *Epidemiol Infect* **133**: 1081-1087.

Harvey RB, Young CR, Ziprin RL, Hume ME, Genovese KJ, Anderson RC *et al*. (1999). Prevalence of *Campylobacter* spp isolated from the intestinal tract of pigs raised in an integrated swine production system. *J Am Vet Med Assoc* **215**: 1601-1604.

Hayashi H, Shibata K, Sakamoto M, Tomita S, Benno Y (2007). *Prevotella copri* sp. nov. and *Prevotella stercorea* sp. nov., isolated from human faeces. *Int J Syst Evol Microbiol* **57**: 941-946.

He G, Shankar RA, Chzhan M, Samouilov A, Kuppusamy P, Zweier JL (1999). Noninvasive measurement of anatomic structure and intraluminal oxygenation in the gastrointestinal tract of living mice with spatial and spectral EPR imaging. *Proc Natl Acad Sci USA* **96**: 4586-4591.

This article has been accepted for publication and undergone full peer review but has not been through the copyediting, typesetting, pagination and proofreading process which may lead to differences between this version and the Version of Record. Please cite this article as an 'Accepted Article', doi: 10.1111/1462-2920.13361

Wiley-Blackwell and Society for Applied Microbiology

Jensen AN, Andersen MT, Dalsgaard A, Baggesen DL, Nielsen EM (2005). Development of real-time PCR and hybridization methods for detection and identification of thermophilic *Campylobacter* spp. in pig faecal samples. *J Appl Microbiol* **99**: 292-300.

Johansson ME, Phillipson M, Petersson J, Velcich A, Holm L, Hansson GC (2008). The inner of the two Muc2 mucin-dependent mucus layers in colon is devoid of bacteria. *Proc Natl Acad Sci USA* **105**: 15064-15069.

Kelly DJ (2001). The physiology and metabolism of *Campylobacter jejuni* and *Helicobacter pylori*. *Symp Ser Soc Appl Microbiol* **30**: 16S-24S.

Konstantinov SR, Awati AA, Williams BA, Miller BG, Jones P, Stokes CR *et al*. (2006). Post-natal development of the porcine microbiota composition and activities. *Environ Microbiol* **8**: 1191-1199.

Korsak D, Maćkiw E, Rożynek E, Żyłowska M (2015). Prevalence of *Campylobacter* spp. in retail chicken, turkey, pork, and beef meat in Poland between 2009 and 2013. *J Food Prot* **78**: 1024-1028.

Lallès JP, Bosi P, Smidt H, Stokes CR (2007). Nutritional management of gut health in pigs around weaning. *Proc Nutr Soc* **66**: 260-268.

Leser TD, Molbak L (2009). Better living through microbial action: the benefits of the mammalian gastrointestinal microbiota on the host. *Environ Microbiol* **11**: 2194-2206.

Looft T, Allen HK, Cantarel BL, Levine UY, Bayles DO, Alt DP *et al*. (2014). Bacteria, phages and pigs: the effects of in-feed antibiotics on the microbiome at different gut locations. *ISME J* **8**: 1566-1576.

Macfarlane GT, Macfarlane LE (2009). Acquisition, evolution and maintenance of the normal gut microbiota. *Dig Dis* **27** (Suppl 1): 90-98.

Macfarlane S, Bahrami B, Macfarlane GT (2011). Mucosal biofilm communities in the human intestinal tract. *Adv Appl Microbiol* **75**: 111-143.

This article has been accepted for publication and undergone full peer review but has not been through the copyediting, typesetting, pagination and proofreading process which may lead to differences between this version and the Version of Record. Please cite this article as an 'Accepted Article', doi: 10.1111/1462-2920.13361

Wiley-Blackwell and Society for Applied Microbiology

Magoč T, Salzberg SL (2011). FLASH: fast length adjustment of short reads to improve genome assemblies. *Bioinformatics* **27**: 2957-2963.

Mahdavi J, Sondén B, Hurtig M, Olfat FO, Forsberg L, Roche N *et al*. (2002). *Helicobacter pylori* SabA adhesin in persistent infection and chronic inflammation. *Science* **297**: 573-578.

Mann E, Schmitz-Esser S, Zebeli Q, Wagner M, Ritzmann M, Metzler-Zebeli BU (2014). Mucosa-associated bacterial microbiome of the gastrointestinal tract of weaned pigs and dynamics linked to dietary calcium-phosphorus. *PLoS One* **9**: e86950.

Marteyn B, Scorza FB, Sansonetti PJ, Tang C (2010). Breathing life into pathogens: the influence of oxygen on bacterial virulence and host responses in the gastrointestinal tract. *Cell Microbiol* **13**: 171-176.

Martin M (2011). Cutadapt removes adapter sequences from high-throughput sequencing reads. *EMBnet.journal* **17.1**: 10-12.

Mayer EA, Tillisch K, Gupta A (2015). Gut/brain axis and the microbiota. *J Clin Invest* **125**: 926-938.

McGuckin MA, Lindén SK, Sutton P, Florin TH (2011). Mucin dynamics and enteric pathogens. *Nat Rev Microbiol* **9**: 265-278.

McMurdie PJ, Holmes S (2013). phyloseq: an R package for reproducible interactive analysis and graphics of microbiome census data. *PLoS One*, **8**: e61217.

Min YW, Rhee PL (2015). The role of microbiota on the gut immunology. *Clin Ther* **37**: 968-975.

Moran ET Jr (2014). Intestinal events and nutritional dynamics predispose *Clostridium perfringens* virulence in broilers. *Poult Sci* **93**: 3028-3036.

This article has been accepted for publication and undergone full peer review but has not been through the copyediting, typesetting, pagination and proofreading process which may lead to differences between this version and the Version of Record. Please cite this article as an 'Accepted Article', doi: 10.1111/1462-2920.13361

Wiley-Blackwell and Society for Applied Microbiology

Naughton JA, Mariño K, Dolan B, Reid C, Gough R, Gallagher ME *et al*. (2013). Divergent mechanisms of interaction of *Helicobacter pylori* and *Campylobacter jejuni* with mucus and mucins. *Infect Immun* **81**: 2838-2850.

Nava GM, Friedrichsen HJ, Stappenbeck TS (2011). Spatial organization of intestinal microbiota in the mouse ascending colon. *ISME J* **5**: 627-638.

Niederer L, Kuhnert P, Egger R, Büttner S, Hächler H, Korczak BM (2012). Genotypes and antibiotic resistances of *Campylobacter jejuni* and *Campylobacter coli* isolates from domestic and travel-associated human cases. *Appl Environ Microbiol* **78**: 288-291.

O' Donnell MM, Harris HM, Jeffery IB, Claesson MJ, Younge B, O' Toole PW *et al*. (2013). The core faecal bacterial microbiome of Irish Thoroughbred racehorses. *Lett Appl Microbiol* **57**: 492-501.

Price MN, Dehal PS, Arkin AP (2009). FastTree: computing large minimum evolution trees with profiles instead of a distance matrix. *Mol Biol Evol* **26**: 1641-1650.

Roeselers G, Mittge EK, Stephens WZ, Parichy DM, Cavanaugh CM, Guillemin K *et al*. (2011). Evidence for a core gut microbiota in the zebrafish. *ISME J* **5**: 1595-1608.

Rotmistrovsky K, Agarwala R (2011). BMTagger: Best Match Tagger for removing human reads from metagenomics datasets. Available at http://www.mmnt.net/db/0/0/ftp.ncbi.nlm.nih.gov/pub/agarwala/bmtagger.

Samuel MC, Vugia DJ, Shallow S, Marcus R, Segler S, McGivern T *et al*. (2004). Epidemiology of sporadic *Campylobacter* infection in the United States and declining trend in incidence, FoodNet 1996-1999. *Clin Infect Dis* **38** (Suppl 3): S165-S174.

Sartor RB, Mazmanian SK (2012). Intestinal microbes in inflammatory bowel diseases. *Am J Gastro Suppl* **1**: 15-21.

Scallan E, Hoekstra RM, Angulo FJ, Tauxe RV, Widdowson MA, Roy SL *et al*. (2011). Foodborne illness acquired in the United States--major pathogens. *Emerg Infect Dis* **17**: 7-15.

Schwarz R, Kaspar A, Seelig J, Künnecke B (2002). Gastrointestinal transit times in mice and humans measured with 27Al and 19F nuclear magnetic resonance. *Magn Reson Med* **48**: 255-261.

Shah HN, Collins DM (1990). *Prevotella*, a new genus to include *Bacteroides melaninogenicus* and related species formerly classified in the genus *Bacteroides*. *Int J Syst Bacteriol* **40**: 205-208.

Shannon CE, Weaver W (1971). The Mathematical Theory of Communication, University of Illinois Press, Urbana, IL.

Silva VL, Carvalho MA, Nicoli JR, Farias LM (2003). Aerotolerance of human clinical isolates of *Prevotella* spp. *J Appl Microbiol* **94**: 701-707.

Stearns JC, Lynch MD, Senadheera DB, Tenenbaum HC, Goldberg MB, Cvitkovitch DG *et al*. (2011). Bacterial biogeography of the human digestive tract. *Sci Rep* **1**: 170.

Sterk A, Schlegel P, Mul AJ, Ubbink-Blanksma M, Bruininx EM (2008). Effects of sweeteners on individual feed intake characteristics and performance in group-housed weanling pigs. *J Anim Sci* **86**: 2990-2997.

Szymanski CM, King M, Haardt M, Armstrong GD (1995). *Campylobacter jejuni* motility and invasion of Caco-2 cells. *Infect Immun* **63**: 4295-4300.

Tam CC, O'Brien SJ, Adak GK, Meakins SM, Frost JA (2003). *Campylobacter coli* - an important foodborne pathogen. *J Infect* **47**: 28-32.

Tap J, Mondot S, Levenez F, Pelletier E, Caron C, Furet JP *et al*. (2009). Towards the human intestinal microbiota phylogenetic core. *Environ Microbiol* **11**: 2574-2584.

Thaiss CA, Zmora N, Levy M, Elinav E (2016). The microbiome and innate immunity. *Nature* **535**: 65-74.

Turnbaugh PJ, Hamady M, Yatsunenko T, Cantarel BL, Duncan A, Ley RE *et al*. (2009). A core gut microbiome in obese and lean twins. *Nature*, **457**: 480-484.

Wang Y, Dong Y, Deng F, Liu D, Yao H, Zhang Q *et al*. (2016). Species shift and multidrug resistance of *Campylobacter* from chicken and swine, China, 2008-14. *J Antimicrob Chemother* **71**: 666-669.

White JR, Nagarajan N, Pop M (2009). Statistical methods for detecting differentially abundant features in clinical metagenomic samples. *PLoS Comput Biol* **5**: e1000352.

Wong S, Waldrop T, Summerfelt S, Davidson J, Barrows F, Kenney PB *et al*. (2013). Aquacultured rainbow trout (*Oncorhynchus mykiss*) possess a large core intestinal microbiota that is resistant to variation in diet and rearing density. *Appl Environ Microbiol* **79**: 4974-4984.

Wright DP, Rosendale DI, Robertson AM (2000). *Prevotella* enzymes involved in mucin oligosaccharide degradation and evidence for a small operon of genes expressed during growth on mucin. *FEMS Microbiol Lett* **190**: 73-79.

Yasuda K, Oh K, Ren B, Tickle TL, Franzosa EA, Wachtman LM *et al*. (2015). Biogeography of the intestinal mucosal and lumenal microbiome in the rhesus macaque. *Cell Host Microbe* **17**: 385-391.

Zhao W, Wang Y, Liu S, Huang J, Zhai Z, He C *et al*. (2015). The dynamic distribution of porcine microbiota across different ages and gastrointestinal tract segments. *PLoS One* **10**: e0117441.

Zoetendal EG, Raes J, van den Bogert B, Arumugam M, Booijink CC, Troost FJ (2012). The human small intestinal microbiota is driven by rapid uptake and conversion of simple carbohydrates. *ISME J* **6**: 1415-1426.

This article has been accepted for publication and undergone full peer review but has not been through the copyediting, typesetting, pagination and proofreading process which may lead to differences between this version and the Version of Record. Please cite this article as an 'Accepted Article', doi: 10.1111/1462-2920.13361

Wiley-Blackwell and Society for Applied Microbiology

Zoetendal EG, von Wright A, Vilpponen-Salmela T, Ben-Amor K, Akkermans AD, de Vos WM (2002). Mucosa-associated bacteria in the human gastrointestinal tract are uniformly distributed along the colon and differ from the community recovered from feces. *Appl Environ Microbiol* **68**: 3401-3407.

This article has been accepted for publication and undergone full peer review but has not been through the copyediting, typesetting, pagination and proofreading process which may lead to differences between this version and the Version of Record. Please cite this article as an 'Accepted Article', doi: 10.1111/1462-2920.13361

Wiley-Blackwell and Society for Applied Microbiology

Figure legends

Fig. 1. Characterisation of the pig mucosa-associated microbiota. (A) Relative contributions (expressed as mean % of total sequence reads) of dominant phyla to the mucosa-associated microbiota along the length of the gastrointestinal tract; (B) Line plot showing changes in relative abundance of dominant phyla along the length of the gastrointestinal tract; (C) Relative abundance of dominant mucosa-associated bacterial families along the length of the gastrointestinal tract. D: duodenum; J: jejunum; I: ileum; C: caecum; PC: proximal colon; DC: distal colon.

Fig. 2. Relative abundance (expressed as % of total sequence reads) of major mucosa-associated bacterial OTUs along the length of the gastrointestinal tract. Values are median ±interquartile range. D: duodenum; J: jejunum; I: ileum; C: caecum; PC: proximal colon; DC: distal colon.

Fig. 3. (A) Principal co-ordinates analysis of weighted UniFrac distances for pig mucosa-associated microbiota calculated and plotted according to small and large intestine; (B) Principal co-ordinates analysis of weighted UniFrac distances calculated and plotted for pig caecal mucosa- and lumenal-associated microbiota.

Fig. 4. Quantitative real-time PCR determination of total 16S rRNA gene copy number in mucosal scrapings along the length of the gastrointestinal tract. Values are median ±interquartile range. Plots that share letters are not significantly different. D: duodenum; J: jejunum; I: ileum; C: caecum; PC: proximal colon; DC: distal colon.

Fig. 5. Changes in relative abundance (expressed as mean % of total sequence reads) of major bacterial families between the caecal mucosa and caecal lumen.

Fig. 6. Differences in relative abundance (expressed as % of total sequence reads) of major bacterial OTUs between the caecal mucosa and lumen. Values are median ±interquartile range. $^{**}P < 0.01$; $^{*}P < 0.05$. CM: caecal mucosa; CL: caecal lumen.

This article has been accepted for publication and undergone full peer review but has not been through the copyediting, typesetting, pagination and proofreading process which may lead to differences between this version and the Version of Record. Please cite this article as an 'Accepted Article', doi: 10.1111/1462-2920.13361

Wiley-Blackwell and Society for Applied Microbiology

Fig. 7. Effect of dietary supplementation with SUCRAM on mucosa-associated microbiota along the length of the gastrointestinal tract. Relative abundance expressed as mean % of total sequence reads. BD: basal diet; BD+S: basal diet + 0.015% (w/w) SUCRAM.

Fig. 8. Effect of SUCRAM on major mucosa-associated bacterial OTUs along the length of the gastrointestinal tract. Relative abundance expressed as % of total sequence reads. Values are median ±interquartile range. D: duodenum; J: jejunum; I: ileum; C: caecum; PC: proximal colon; DC: distal colon.

Fig. 9. Calculated 16S rRNA gene copy number for mucosa-associated *Campylobacter coli*-OTU3063 in duodenum and jejunum in response to dietary supplementation with SUCRAM. Values are median ±interquartile range. ***$P < 0.001$.

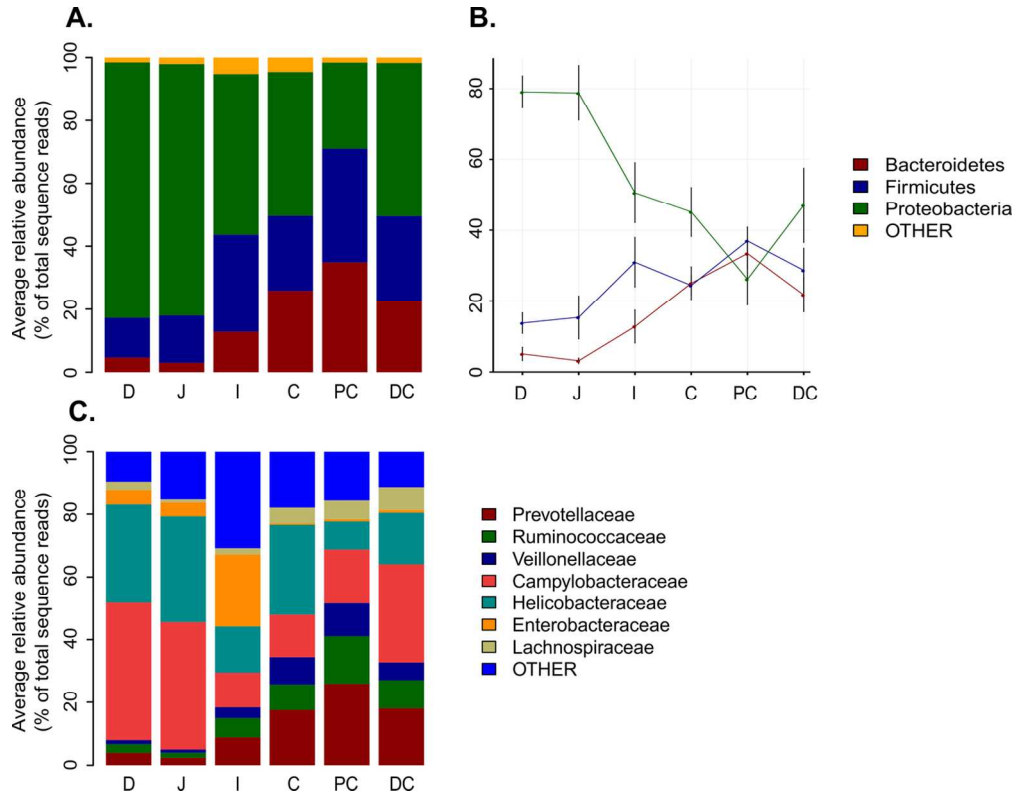

Fig. 1. Characterisation of the pig mucosa-associated microbiota. (A) Relative contributions (expressed as mean % of total sequence reads) of dominant phyla to the mucosa-associated microbiota along the length of the gastrointestinal tract; (B) Line plot showing changes in relative abundance of dominant phyla along the length of the gastrointestinal tract; (C) Relative abundance of dominant mucosa-associated bacterial families along the length of the gastrointestinal tract. D: duodenum; J: jejunum; I: ileum; C: caecum; PC: proximal colon; DC: distal colon.

127x99mm (300 x 300 DPI)

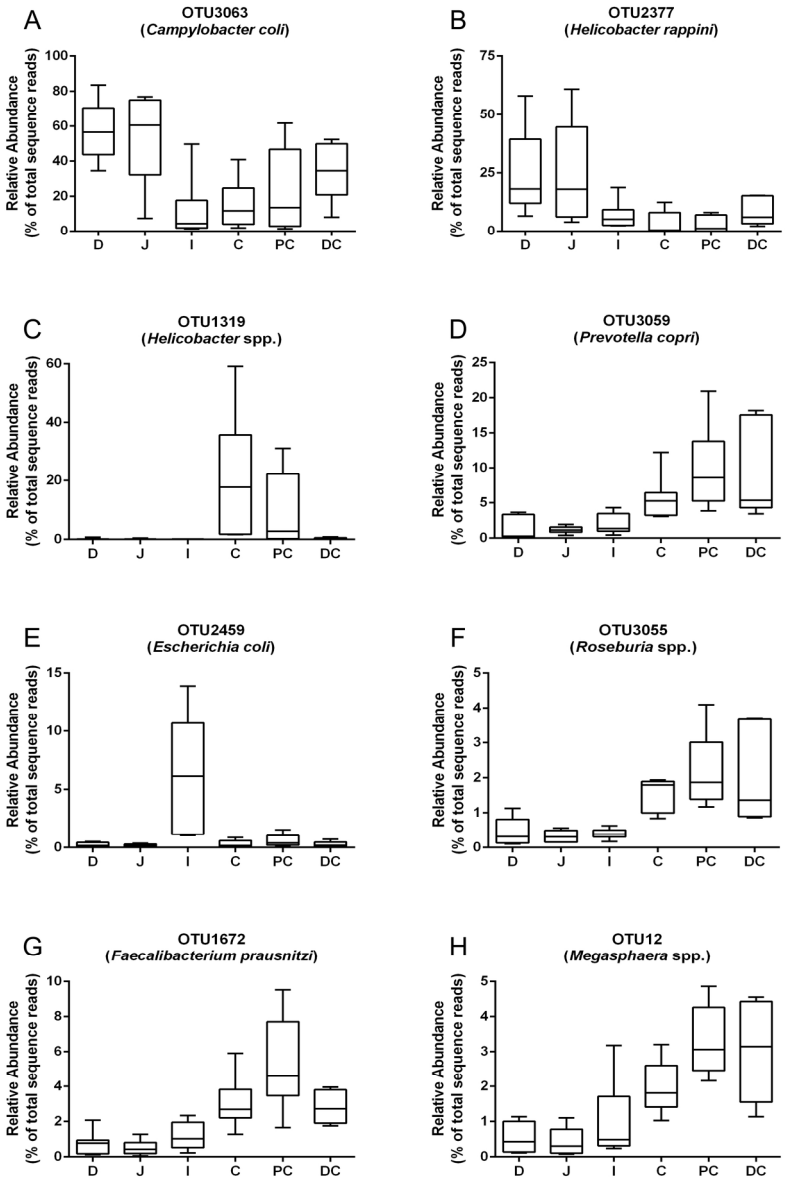

Fig. 2. Relative abundance (expressed as % of total sequence reads) of major mucosa-associated bacterial OTUs along the length of the gastrointestinal tract. Values are median ±interquartile range. D: duodenum; J: jejunum; I: ileum; C: caecum; PC: proximal colon; DC: distal colon.

163x235mm (300 x 300 DPI)

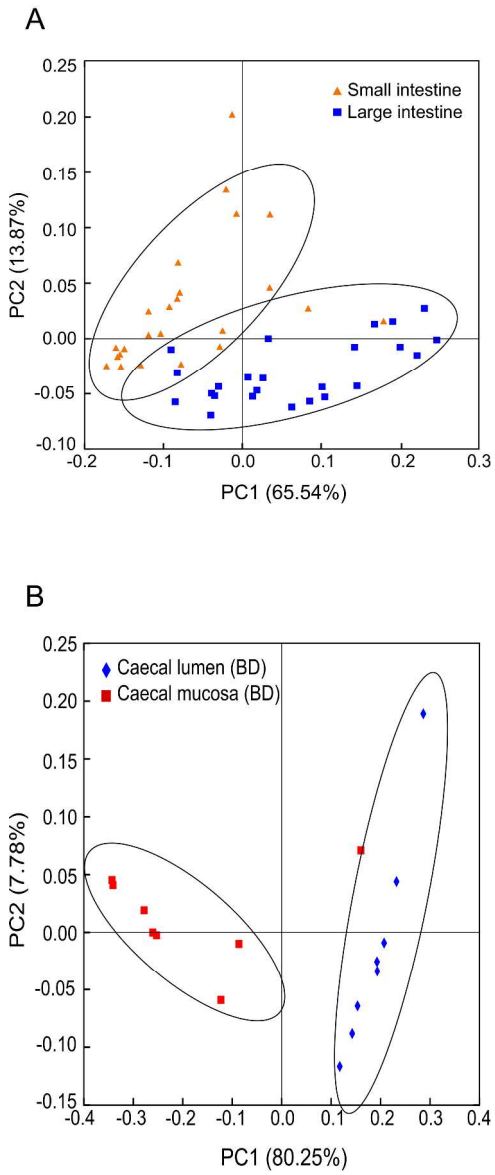

Fig. 3. (A) Principal co-ordinates analysis of weighted UniFrac distances for pig mucosa-associated microbiota calculated and plotted according to small and large intestine; (B) Principal co-ordinates analysis of weighted UniFrac distances calculated and plotted for pig caecal mucosa- and lumenal-associated microbiota.

231x577mm (300 x 300 DPI)

This article has been accepted for publication and undergone full peer review but has not been through the copyediting, typesetting, pagination and proofreading process which may lead to differences between this version and the Version of Record. Please cite this article as an 'Accepted Article', doi: 10.1111/1462-2920.13361

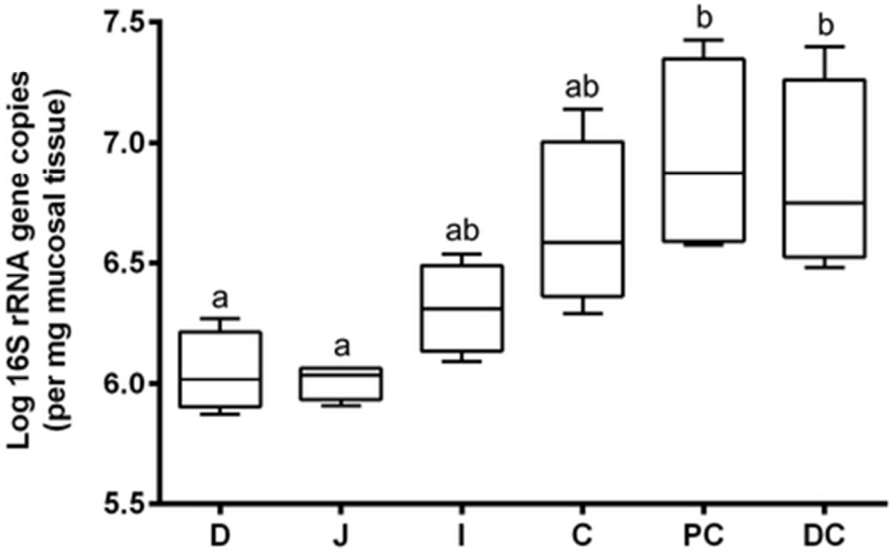

Fig. 4. Quantitative real-time PCR determination of total 16S rRNA gene copy number in mucosal scrapings along the length of the gastrointestinal tract. Values are median ±interquartile range. Plots that share letters are not significantly different. D: duodenum; J: jejunum; I: ileum; C: caecum; PC: proximal colon; DC: distal colon.

42x26mm (300 x 300 DPI)

This article has been accepted for publication and undergone full peer review but has not been through the copyediting, typesetting, pagination and proofreading process which may lead to differences between this version and the Version of Record. Please cite this article as an 'Accepted Article', doi: 10.1111/1462-2920.13361

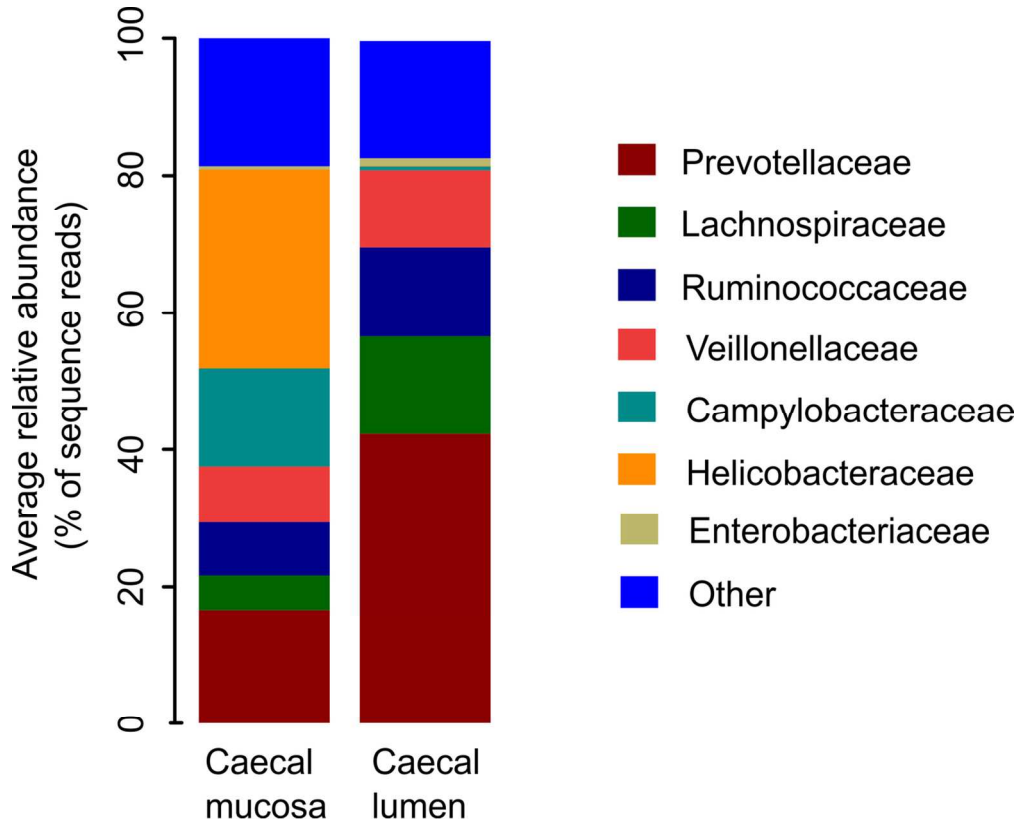

Fig. 5. Changes in relative abundance (expressed as mean % of total sequence reads) of major bacterial families between the caecal mucosa and caecal lumen.

124x100mm (300 x 300 DPI)

This article has been accepted for publication and undergone full peer review but has not been through the copyediting, typesetting, pagination and proofreading process which may lead to differences between this version and the Version of Record. Please cite this article as an 'Accepted Article', doi: 10.1111/1462-2920.13361

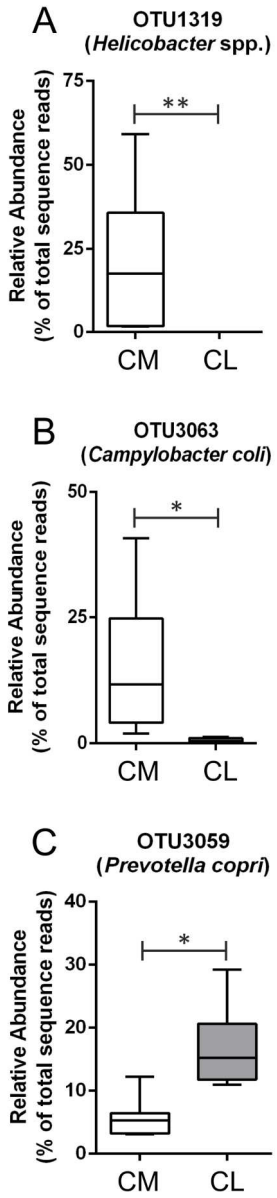

Fig. 6. Differences in relative abundance (expressed as % of total sequence reads) of major bacterial OTUs between the caecal mucosa and lumen. Values are median ±interquartile range. **P < 0.01; *P < 0.05. CM: caecal mucosa; CL: caecal lumen.

105x422mm (300 x 300 DPI)

This article has been accepted for publication and undergone full peer review but has not been through the copyediting, typesetting, pagination and proofreading process which may lead to differences between this version and the Version of Record. Please cite this article as an 'Accepted Article', doi: 10.1111/1462-2920.13361

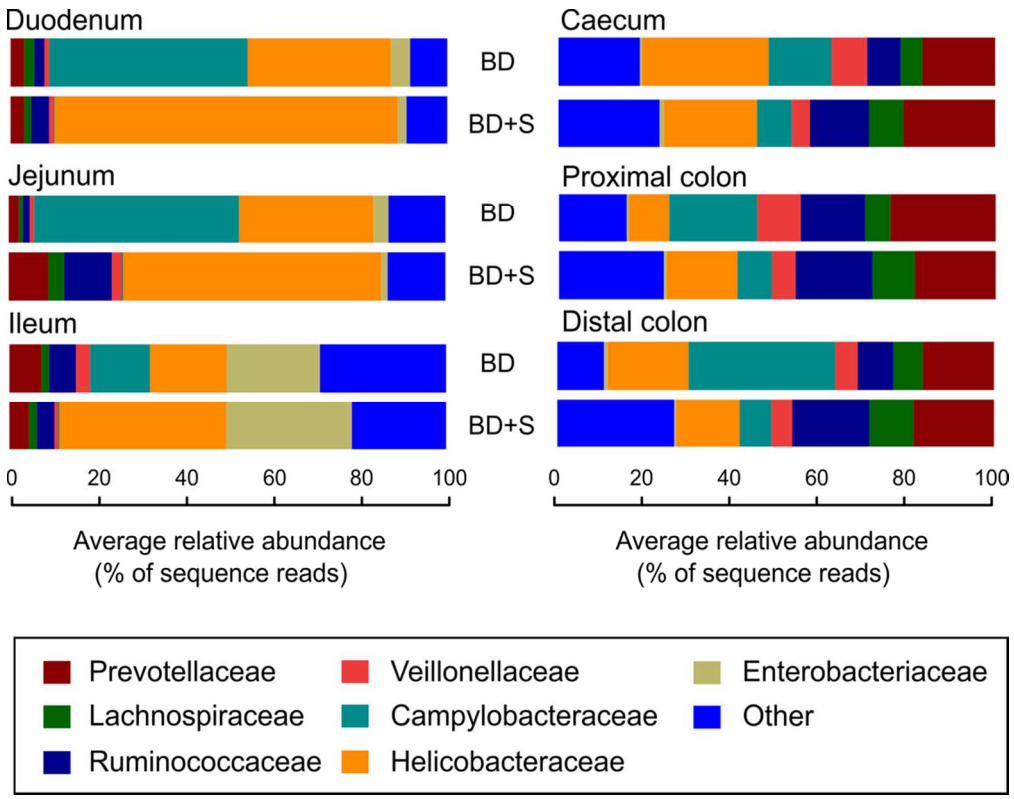

Fig. 7. Effect of dietary supplementation with SUCRAM on mucosa-associated microbiota along the length of the gastrointestinal tract. Relative abundance expressed as mean % of total sequence reads. BD: basal diet; BD+S: basal diet + 0.015% (w/w) SUCRAM.

97x76mm (300 x 300 DPI)

This article has been accepted for publication and undergone full peer review but has not been through the copyediting, typesetting, pagination and proofreading process which may lead to differences between this version and the Version of Record. Please cite this article as an 'Accepted Article', doi: 10.1111/1462-2920.13361

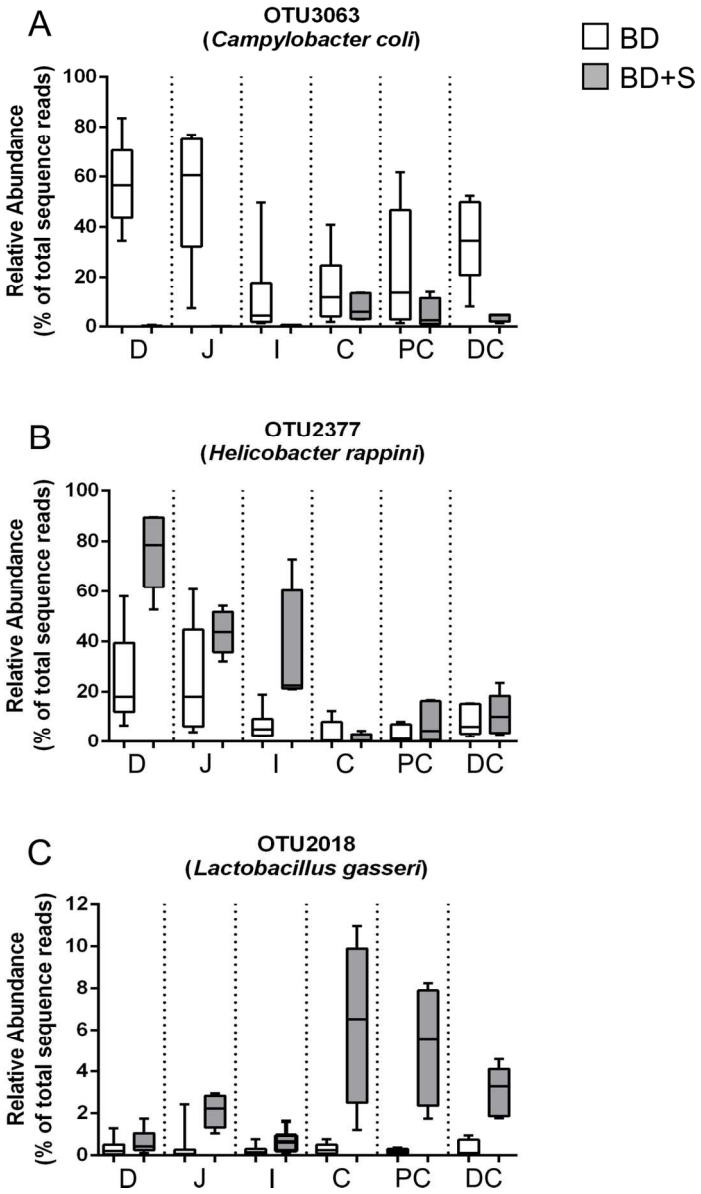

Fig. 8. Effect of SUCRAM on major mucosa-associated bacterial OTUs along the length of the gastrointestinal tract. Relative abundance expressed as % of total sequence reads. Values are median ±interquartile range. D: duodenum; J: jejunum; I: ileum; C: caecum; PC: proximal colon; DC: distal colon.

110x186mm (300 x 300 DPI)

This article has been accepted for publication and undergone full peer review but has not been through the copyediting, typesetting, pagination and proofreading process which may lead to differences between this version and the Version of Record. Please cite this article as an 'Accepted Article', doi: 10.1111/1462-2920.13361

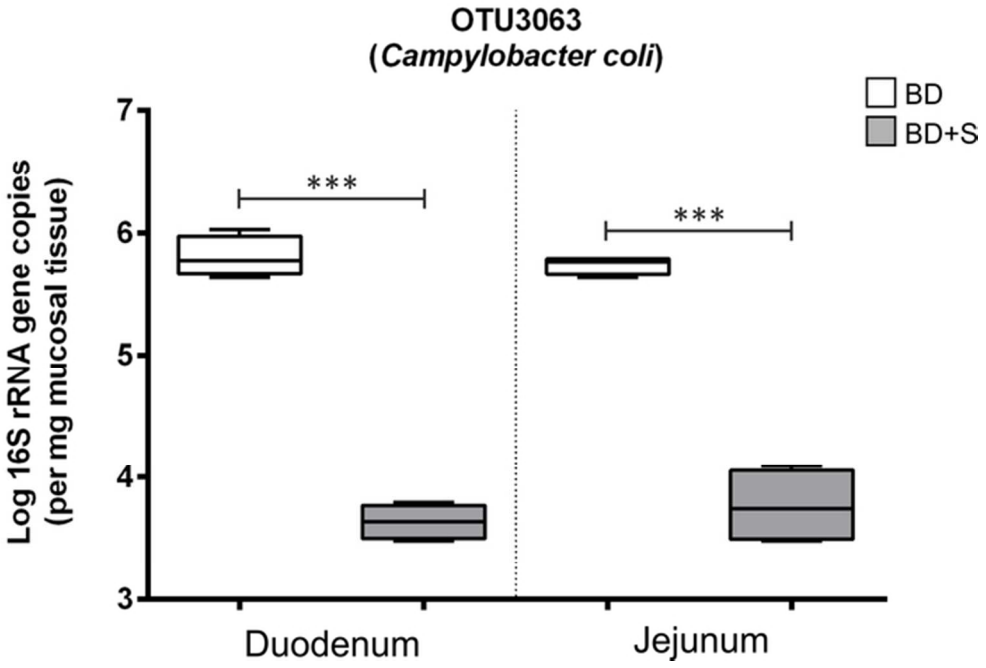

Fig. 9. Calculated 16S rRNA gene copy number for mucosa-associated Campylobacter coli-OTU3063 in duodenum and jejunum in response to dietary supplementation with SUCRAM. Values are median ±interquartile range. ***P < 0.001.

60x41mm (300 x 300 DPI)

This article has been accepted for publication and undergone full peer review but has not been through the copyediting, typesetting, pagination and proofreading process which may lead to differences between this version and the Version of Record. Please cite this article as an 'Accepted Article', doi: 10.1111/1462-2920.13361